DEVELOPMENTAL DYNAMICS 235:2567–2573, 2006

SPECIAL ISSUE PATTERNS & PHENOTYPES

Comparative Expression of Mouse and Chicken Shisa Homologues During Early Development

Mário Filipe,[1†] Lisa Gonçalves,[1,2†] Margaret Bento,[1,2†] Ana Cristina Silva,[1,2] and José António Belo[1,2*]

During vertebrate embryogenesis, fibroblast growth factor (FGF) and Wnt signaling have been implicated in diverse cellular processes, including cell growth, differentiation, and tissue patterning. The recently identified *Xenopus* Shisa protein promotes head formation by inhibiting Wnt and FGF signaling through its interaction with the immature forms of Frizzled and FGF receptors in the endoplasmic reticulum, which prevents their posttranslational maturation. Here, we describe the mouse and chicken homologues of *Xenopus* Shisa. The mouse and chicken Shisa proteins share, respectively, 33.6% and 33.8% identity with the *Xenopus* homolog. In situ hybridization analysis shows that mouse *shisa* is expressed throughout embryonic development, predominantly in the anterior visceral endoderm, headfolds, somites, forebrain, optic vesicle, and limb buds. Cross-species comparison shows that the expression pattern of *cshisa* closely mirrors that of *mshisa*. Our observations indicate that the Shisa family genes are typically expressed in tissues known to require the modulation of Wnt and FGF signaling. *Developmental Dynamics 235:2567–2573, 2006.*

Key words: mouse; chicken; shisa; presomitic mesoderm; somite; anterior visceral endoderm; limb buds

Accepted 30 April 2006

INTRODUCTION

The establishment of the anteroposterior (AP) axis in vertebrates has been postulated to be under the control of two distinct head and trunk organizing centers (Spemann, 1931; Mangold, 1933). In mammals, the head-inducing activity is thought to reside in the anterior visceral endoderm (AVE) and later in the axial mesendoderm, whereas trunk-inducing and patterning activities reside in the more posterior primitive streak/node (Belo et al., 1997; Bouwmeester and Leyns, 1997; Beddington and Robertson, 1999).

The AVE is an extraembryonic tissue required for early anterior neural specification in the mouse embryo (Thomas and Beddington, 1996). The AVE is induced at the distal tip of the 5.5 days postcoitum (dpc) embryo and then migrates to the prospective anterior side, where it imparts anterior identity upon the underlying epiblast (Rivera-Perez et al., 2003; Yamamoto et al., 2004; Srinivas et al., 2004; Rodriguez et al., 2005).

Signaling molecules play crucial roles in developmental events, and their actions are highly regulated by endogenous modulators and antagonists to obtain precisely balanced outputs. The process of neural AP patterning involves the integration of various signals such as retinoic acid (RA), fibroblast growth factors (FGF), and members of the Wnt family. The combined inhibition of bone morphogenetic protein-4 (BMP4), Nodal, and Wnt8 signaling has been demonstrated to be necessary for the specification of anterior neural tissues (Glinka et al., 1997; Piccolo et al., 1999; Silva et al., 2003). Several secreted antagonists of the BMP, Nodal, and Wnt pathways, such as Cerl, Lefty1, and Dkk-1, are expressed in the mouse AVE underlying the prospective anterior neuroectoderm (Belo et al., 1997; Glinka et al., 1998; Ould-Abdelghani et al., 1998). Likewise, the

[1]Instituto Gulbenkian de Ciência, Oeiras, Portugal
[2]Centro de Biomedicina Molecular e Estrutural, Universidade do Algarve, Campus de Gambelas, Faro, Portugal
[†]Drs. Filipe, Gonçalves, and Bento contributed equally to this work.
***Correspondence to: José A. Belo, Centro de Biomedicina Molecular e Estrutural, Universidade do Algarve, Campus de Gambelas, 8005-139 Faro, Portugal. E-mail: jbelo@ualg.pt**

DOI 10.1002/dvdy.20862
Published online 13 June 2006 in Wiley InterScience (www.interscience.wiley.com).

acknowledged topological and functional equivalent of the AVE in chick, the hypoblast, also expresses Nodal, BMP, and Wnt antagonists, such as Caronte, Dkk-1, and Crescent (Pfeffer et al., 1997; Rodriguez Esteban et al., 1999; Foley et al., 2000).

Development of the vertebrate limb bud involves a series of cell and axis specification and patterning processes directed by specialized structures such as the zone of polarizing activity (ZPA), the apical ectodermal ridge (AER), and the nonridge ectoderm. The organizing and patterning activities of these regions are mediated by specific genes that have been shown to be regulated by a complex network of transforming growth factor-beta (TGF-β), BMP, FGF, and Wnt signaling pathways (reviewed in Capdevila and Izpisua Belmonte, 2001). FGFs expressed in the AER, such as FGF2, 4, and 8, promote the proliferation of the mesenchymal limb bud cells in the progress zone and are absolutely required for limb outgrowth. Wnt3A, initially expressed in the limb surface ectoderm and subsequently restricted to the AER cells, plays an essential role in controlling the induction of the AER. Another Wnt factor, Wnt7A, is expressed in the dorsal ectoderm and is involved in the specification of dorsal identities in the limb. FGFs also have been shown to oppose TGF-β2–induced chondrogenesis, and this inhibition is necessary to keep the proliferating mesenchymal cells of the progress zone in an undifferentiated state and maintain limb outgrowth. A strong argument can be made, therefore, for the important role that modulation mechanisms for such signaling pathways must play in the positioning and outgrowth of the limbs.

Metameric organization of the vertebrate body plan is established by somitogenesis, a process by which the paraxial mesoderm becomes segmented into somites, which later will give rise to the vertebrae, skeletal muscles, and part of the dermis (reviewed in Pourquie, 2001). Wnt and FGF signaling pathways are key elements in almost all steps of this process. Correct specification of paraxial mesoderm, a prerequisite event for somitogenesis, is dependent on Wnt and FGF patterning signals (Deng et al., 1994; Yoshikawa et al., 1997; Sun et al., 1999). The precise spatial and temporal formation of somites relies on the concerted action of two major mechanistic components: the segmentation clock, a molecular oscillator that drives the cyclic expression of a set of genes, setting the periodicity of somite formation; and the determination front, a dynamic morphogen gradient that confers positional responsiveness of the presomitic mesoderm (PSM) cells to the clock signals, thereby defining the segmentation boundaries (reviewed in Pourquie, 2004; Dubrulle and Pourquie, 2004a; Aulehla and Herrmann, 2004). Progression of the determination front involves the establishment of a caudorostral gradient of FGF8/Wnt3A activities along the PSM (Dubrulle et al., 2001; Aulehla et al., 2003; Dubrulle and Pourquie, 2004b). Furthermore, evidence suggests that the oscillations in notch signaling, which controls the expression of cyclic genes linked to the segmentation clock, are dependent on Wnt3A in the posterior PSM (Aulehla et al., 2003). The formed somites undergo a maturation process in response to signals emerging from surrounding structures, which leads to the differentiation of three compartments: the sclerotome, the myotome, and the dermatome. The sclerotome gives rise to the vertebrae and ribs and forms from a ventromedial epithelium that has acquired mesenchymal character. The dorsolateral epithelium that remains forms a cap, the dermomyotome, gives rise to the dermatome, from which the dorsal skin dermis originates, and to the myotome, which will form skeletal muscle. Instructive Wnt and FGF signals, among others, are responsible for the specification of the different cell fates in the somite. Particularly, Wnt signaling from the dorsal neural tube and adjacent ectoderm (Stern and Hauschka, 1995; Wagner et al., 2000) and FGFs from the somite itself (Crossley and Martin, 1995; Grass et al., 1996; Pirskanen et al., 2000) have an important role in the specification and maintenance of myogenic fates.

A recently described *Xenopus* protein termed Shisa, was shown to promote head formation through the inhibition of both Wnt and FGF signaling pathways by a novel ER retention mechanism (Yamamoto et al., 2005). Secreted antagonists that competitively bind to caudalizing/ventralizing factors (Piccolo et al., 1996, 1999; Zimmerman et al., 1996) or to their receptors preventing ligand binding (Mao et al., 2001) play a major role in the head-inducing activity of the organizer. However, Shisa, which is expressed in the organizer and anterior endomesoderm as well as in the anterior neuroectoderm, is able to inhibit Wnt and FGF signals in a cell-autonomous manner. It does so by physically interacting with the immature forms of the Wnt and FGF receptors within the ER and preventing their posttranslational modification and trafficking to the cell surface (Yamamoto et al., 2005).

Here, we report the identification of the mouse and chicken homologues of *Xenopus* Shisa. We present a detailed description of the expression patterns of *mshisa* and *cshisa* during mouse and chick development and compare them with *Xshisa* expression in *Xenopus*.

RESULTS AND DISCUSSION

Cloning and Sequence Analysis of Mouse and Chicken *shisa*

To gain further insight into the molecular mechanisms involved in the early steps of forebrain specification, we have carried out a screening for differentially expressed genes in the mouse AVE (Filipe et al., unpublished results). Briefly, a transgenic mouse line was generated in which enhanced green fluorescent protein (EGFP) is expressed in the AVE, under the control of the promoter region of the Cerl gene (TgN(Cerl-GFP)328Belo; Mesnard et al., 2004). In this transgenic line, the AP axis reorientation could be followed, by the fluorescently labeled AVE cells, even before gastrulation. Gene expression profiling using GeneChips (Affymetrix) identified several new transcripts expressed in the AVE at the very early stages of AP axis establishment.

One of the novel genes identified in this screening and provisory named MAd2 (Mouse Anterodistally expressed gene 2, probe set ID 1423852_at), was found to display a

particularly interesting dynamic expression pattern that warranted a more detailed analysis. A BLAST search (Altschul et al., 1990) of the *Xenopus laevis* expressed sequence tag (EST) database using the MAd2 sequence as query, returned a potential homolog, which was reported recently by Yamamoto et al. (2005) as *shisa*. In view of this finding, the MAd2 gene was henceforth designated as mouse *shisa* (GenBank accession no. DQ342342). The EST clone BC057640, obtained from RZPD (IMAGp998G149268Q3), was sequenced and found to contain the entire putative coding sequence (CDS) of *mshisa* as well as 5′ and 3′ untranslated regions (UTRs). This putative CDS consists of an 888-bp open reading frame (ORF) that encodes a predicted 295-amino acid protein with a calculated molecular weight of 31.6 kDa, whose sequence is identical to that reported by Yamamoto et al. (2005) for the mouse Shisa homolog.

The cDNA sequence of *mshisa* was then used to Blast the *Gallus gallus* sequence databases for potential homologs. This search led to the identification of two mRNAs (GenBank accession no. NM_204501, AF257354) and three EST clones (GenBank accession no. DR424805, BU205915, BM488505). An 855-bp ORF from the AF257354 RNA was identified as the putative *cshisa* CDS, which encodes for a 284-amino acid protein with a predicted molecular weight of 29.9 kDa. The *cshisa* cDNA sequence was then assembled in silico from the retrieved sequences and submitted to GenBank with the accession no. DQ342343.

Sequence comparison of the Shisa homologs reveals two highly conserved cysteine-rich domains (CRD; Fig. 1). The three proteins are also relatively well conserved over their entire sequence, with the murine and chicken Shisa showing, respectively, 33.6% and 33.8% overall identity and 49.5% and 49.2% overall similarity to the *Xenopus* protein. The Shisa proteins of the two amniote vertebrates are even more closely related to each other, sharing 81% identity and 85.8% similarity.

The gene structure of the mouse and chicken *shisa* was deduced from cDNA-genomic alignments and by using the Genscan gene prediction program (http://genes.mit.edu/GENSCAN.html; Burge and Karlin, 1997). The mouse *shisa* gene is composed of two exons, each containing one of the CRDs and separated by a 3,234-bp phase 1 intron, inserted between the first and second base of the codon for the first valine in the conserved sequence VPIYVPFLIV. An identical two-exon gene structure was reported for two other mammalian homologs, the rat and human *shisa* (Katoh and Katoh, 2005). Despite the still preliminary nature of the first draft of the chicken genome assembly, which did not allow the unequivocal determination of the exon structure of the *cshisa* gene, it was nevertheless possible to identify a 1,140-bp intron placed at the exactly same position as the mouse *shisa* intron. Another evidence supporting the homology of the murine and chicken *shisa* comes from the chromosomal location of these two genes, which map to syntenic regions in the mouse chromosome 14C3 and chicken chromosome 1, as annotated in the Ensembl genome databases (v.37 - Feb2006; http://www.ensembl.org/; Birney et al., 2006).

Expression of *mshisa* During Mouse Development

In situ hybridization analysis was used to examine the expression of *mshisa* transcripts during mouse embryogenesis. The expression of *mshisa* can be seen as early as 5.5 dpc and continues throughout embryonic development (Fig. 2). At pre- to early streak stages, *mshisa* is specifically expressed in the AVE as it migrates to the anterior side (Fig. 2A–C). By late streak stage, expression is found in a patch of anterior definitive endoderm (ADE) cells that has replaced the AVE (Fig. 2D).

In early allantoic bud embryos (Fig. 2E), around embryonic day (E) 7.25–E7.5, *mshisa* transcripts can only be detected in the ADE and subjacent cranial mesoderm (Fig. 2E′–E‴), while by early headfold stage, *mshisa* is also induced in the anterior neural plate (Fig. 2F′). Up to this point, *mshisa* expression seems to be excluded from the midline axial mesendoderm (Fig. 2F). As the embryo reaches stage E8.0, *mshisa* is expressed in the cephalic mesenchyme and presumptive forebrain neuroectoderm (Fig. 2G–G″). Expression is also present in the endoderm lining the foregut pocket and in the rostral end of the notochordal plate (Fig. 2G″).

By E8.5, *mshisa* expression marks the prospective eye and forebrain regions (Fig. 2H–H″). Expression of *mshisa* is maintained in the optic vesicles of E9.0–E9.5 embryos (Fig. 2I–I′,J), and the same is true for the expression in the forebrain, which can be more precisely located to the surface ectoderm and neuroepithelium of the prosencephalic vesicle (Fig. 2J′). Other expression domains found at this stage include the pharyngeal pouches (Fig. 2J), the lateral region of the invaginating otic pit (Fig. 2H″,I′), and the ventral endoderm of the foregut and immediately adjacent mesenchyme (Fig. 2J′). Later in development, *mshisa* expression in the forebrain appears to become progressively confined to the dorsal telencephalon (Fig. 2K).

With the onset of somitogenesis, *mshisa* starts to be expressed in the forming somites, but is apparently absent from the presomitic mesoderm (Fig. 2H–K). Somitic expression of *mshisa* is restricted to the dorsolateral part that constitutes the dermomyotome (Fig. 2I″,K′). This expression pattern persists through later stages, albeit gradually decreasing to lower levels in older somites (Fig. 2H–K).

Expression of *mshisa* in the developing limb buds can first be seen in a proximal domain (arrowhead, Fig. 2K) that subsequently shifts toward the distal tip as the bud grows (Fig. 2L). The expression in the limb bud is restricted to the ectoderm, as shown in Figure 2L′. At E13.5, *mshisa* expression can still be detected in the tip of the forming digits (Fig. 2M), in the region undergoing chondrogenesis.

Expression of *cshisa* During Chick Development

Embryos from prestreak to mid-limb stages of development (Hamburger and Hamilton, 1951) were examined by in situ hybridization (Fig. 3). Our observations reveal that the expression pattern of *cshisa* is very similar to that of its murine counterpart.

At prestreak stages (Hamburger

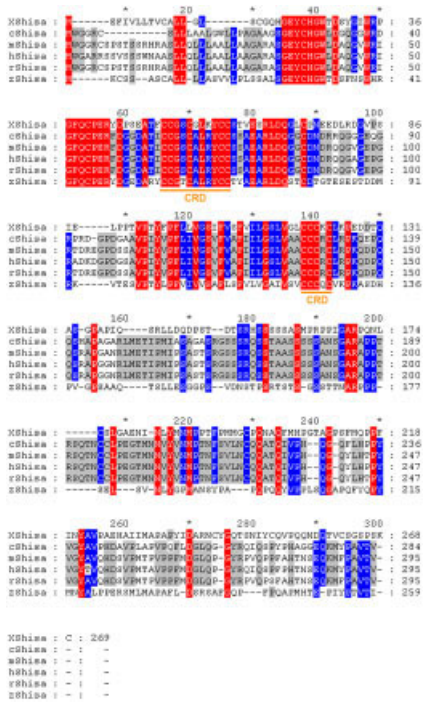

Fig. 1. Sequence alignment of XShisa, cShisa, mShisa, rShisa, hShisa, and zShisa. Predicted amino acid sequences of cysteine-rich domains are underlined in orange. Identical amino acids among all are shaded red, whereas identical amino acids in only two sequences are shaded blue.

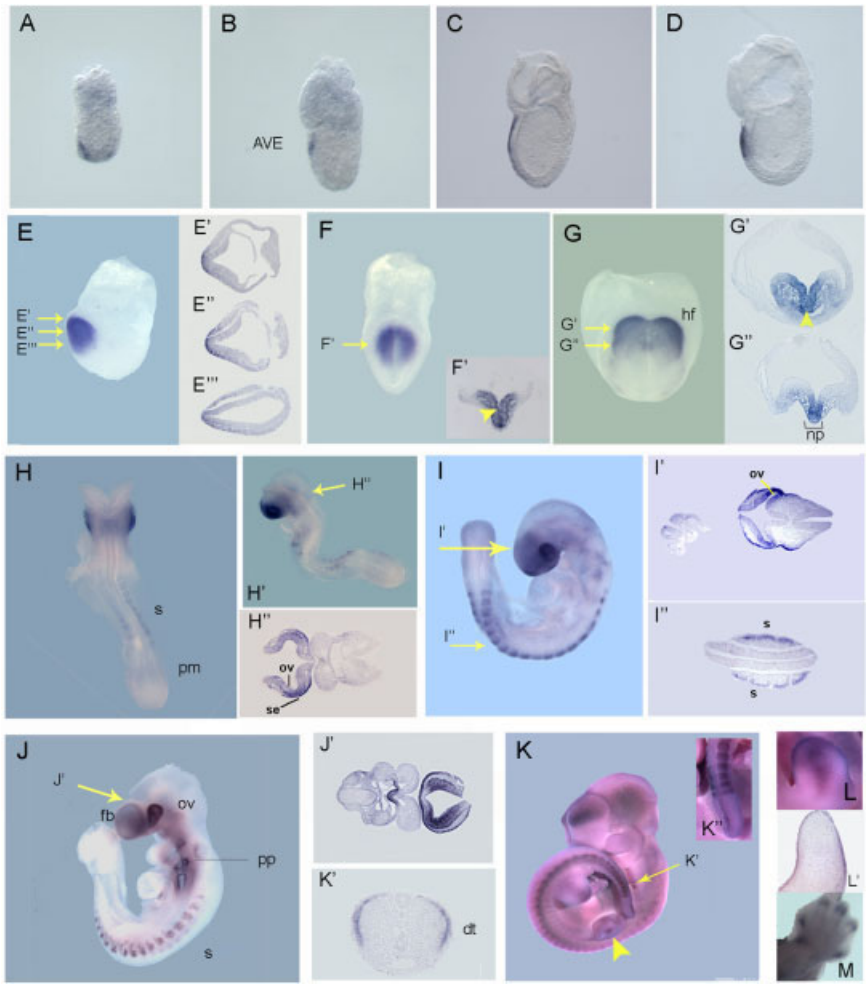

Fig. 2.

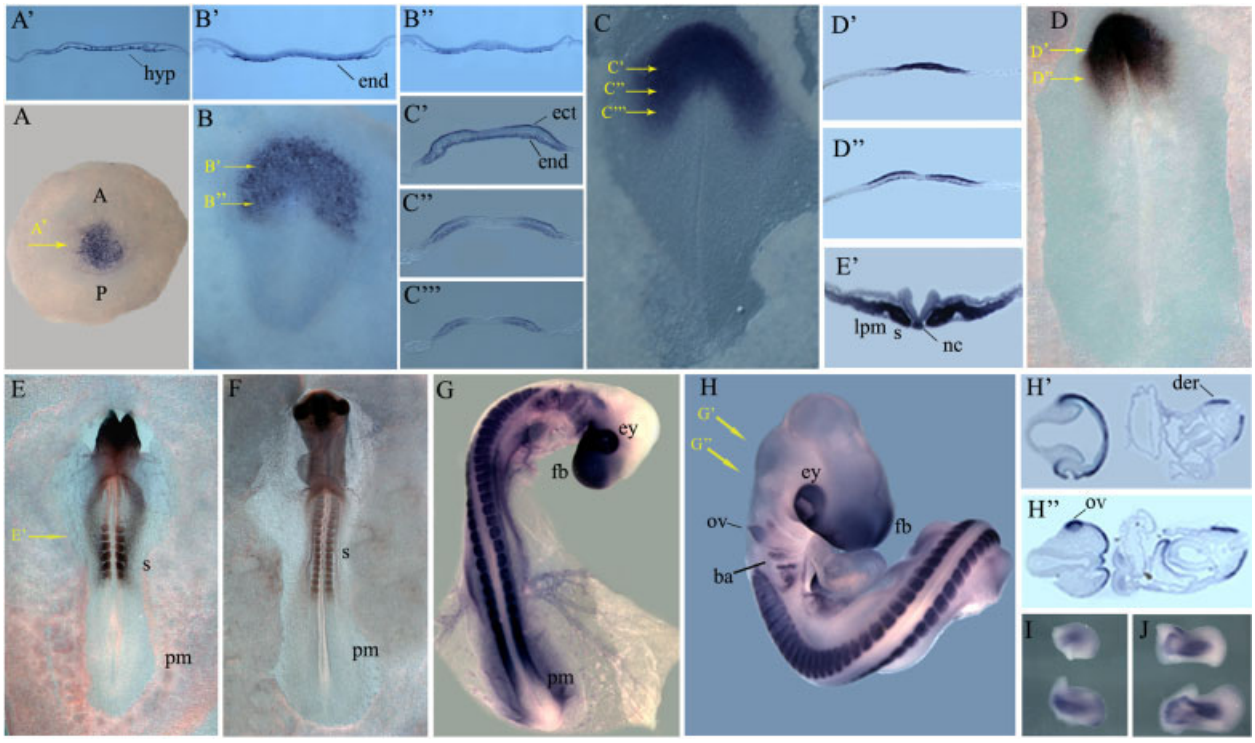

Fig. 3.

and Hamilton stage 1, HH1), *cshisa* transcripts were strongly detected in the hypoblast (Fig. 3A,A′). As gastrulation begins and the primitive streak is formed, *cshisa* expression becomes restricted to the anterior part of the embryo, more specifically to the endodermal layer (stage HH3$^+$; Fig. 3B,B′,B″). By stage HH5 (Fig. 3C), *cshisa* is expressed in the prospective neural plate tissue. Transverse sections showed that *cshisa* transcripts are still present in the endodermal layer and also start to be expressed in mesodermal cells (Fig. 3C′,C″,C‴). This expression pattern is consistent with the observation that *Xshisa* is essential for vertebrate head formation (Yamamoto et al., 2005). At stage HH6, *cshisa* mRNA is present in high levels in the head folds and neural plate region (Fig. 3D). Transverse sections show that *cshisa* transcripts are localized to the ectodermal cells (Fig. 3D′,D″).

With the beginning of somitogenesis, *cshisa* starts also to be expressed in the somitic territories. At stage HH7, *cshisa* can be detected in the first forming somite (not shown). By stage HH9$^-$ *cshisa* is strongly expressed in the head folds and in the developing somites (Fig. 3E). A dynamic expression pattern is observed throughout somitogenesis (Fig. 3E–H). *cshisa* transcripts are absent from the posterior region of the presomitic mesoderm but can be detected at low levels at its rostral end. The expression is strongest in the newly formed somites and gradually decreases as the somites mature. A transverse section at the somite level of a stage HH7 embryo shows that *cshisa* is expressed in the entire somite as well as in the lateral plate mesoderm and notochord (Fig. 3E′). Later in development, *cshisa* transcripts are also present in the prospective eye, forebrain, branchial arches, and otic vesicle (Fig. 3F–H). As the optic vesicles evaginate, expression is seen in the lens vesicle and anterior surface ectoderm of the frontonasal mass (Fig 3H–H″). At stage HH25, *cshisa* expression in the somite is restricted to the dermomyotome (Fig. 3H′,H″), resembling that of *mshisa* (Fig. 2K′).

During early limb bud stages, *cshisa* starts to be detected in the more proximal region of the limb buds (not shown) and later, as limbs develop, the expression shifts toward the distal region (Fig. 3I,J). This expression pattern in the limb buds resembles the one observed for *MyoD*, a marker of differentiating myogenic cells (Gamer et al., 2001; Fig. 3I,J).

As demonstrated above, the murine and chicken *shisa* are very closely related to each other both in terms of their sequence similarity and the evolutionarily conserved expression pattern. The early expression of *mshisa* and *cshisa* in the AVE/hypoblast and anterior neuroectoderm also recapitulates the deep endomesoderm and prospective head ectoderm expression previously described for the *Xenopus shisa*, the founding member of this gene family (Yamamoto et al., 2005). Mouse and chicken *shisa*, however, additionally are expressed in structures such as the somites, pharyngeal region. and the eye.

Being members of the *Xshisa* family, an antagonist of Wnt and FGF signalling (Yamamoto et al., 2005), the conserved expression patterns of both *mshisa* and *cshisa* reflect the im-

Fig. 2. Expression pattern of *mshisa* during mouse development. Analysis performed by in situ hybridization. All sections are 8 μm thick. The level at which each section was taken is indicated on panels with yellow arrows, and the sections are shown next to the relevant panels. **A–D:** *mshisa* is expressed in the AVE in embryonic day (E) 5.5, E6.5, E6.75, and E7.0 mouse embryos. **E:** At E7.25 *mshisa* is detected in the prospective head fold. **E′,E″, E‴:** Transverse sections of an E7.25 embryo show that *mshisa* is only expressed in the anterior definitive endoderm and subjacent cranial mesoderm. **F:** In an E7.5 embryo, *mshisa* is expressed in the head folds. F′: Transverse section of E7.5 embryo shows that *mshisa* is also induced in the anterior neural plate. **G:** In an E8.0 embryo, *mshisa* is expressed in the head folds. Transverse sections show that mshisa is present in the cephalic mesenchyme, in the presumptive forebrain neuroectoderm, in the endoderm lining the foregut pocket (G′) and in the rostral end of the notochordal plate (G″). **H,H′:** At E8.5 *mshisa* transcripts are expressed in the prospective eye, forebrain, and somites. H″: Transverse section of E8.0 embryo shows that *mshisa* is expressed in the optic pit and surface ectoderm. **I:** At E9.0, *mshisa* is expressed in the eye, somites, and forebrain. **I′,I″:** Transverse sections of an E9.0 embryo show expression of *mshisa* in the optic vesicle, optic eminence, and somites. **J:** At E9.5, *mshisa* is expressed in the eye, forebrain, somites, and pharyngeal pouches. **J′:** Transverse section shows that *mshisa* is present in the surface ectoderm and in the ventral endoderm of the foregut and immediately adjacent mesenchyme. **K:** At E11.5, transcripts of *mshisa* are expressed in the dorsal telencephalon, in the eye, in the somites, and limb buds. **K′:** Transverse section of the tail at E11.5 shows *mshisa* in the somite is restricted to the dermomyotome. **K″:** Amplification of the tail shows that *mshisa* is absent from the presomitic mesoderm. **L:** Amplification of the limb bud at E11.5 shows *mshisa* expression. **L′:** Sagittal section of the limb bud at E11.5 shows that *mshisa* expression is restricted to the surface ectoderm. K: Amplification of the limb at 13.5 shows *mshisa* is detected in the tip of the forming digits. AVE, anterior visceral endoderm; dt, dermatome; fb, forebrain; fg, foregut; hf, head fold; np, notochordal plate; ov, optic vesicle; pm, presomitic mesoderm; pp, pharyngeal pouches; s, somite; se, surface ectoderm.

Fig. 3. Localization of cshisa transcripts in developing chicken embryos detected by in situ hybridization. A, C, E and F are ventral views, whereas B and D are dorsal views of whole-mount embryos. All sections are transverse 16-μm cryo-sections. The level at which each section was taken is indicated on panels with yellow arrows, and the sections are shown next to the relevant panels. **A:** *cshisa* is expressed in the hypoblast in Hamburger and Hamilton stage (HH) 1 chicken embryo. Anterior is to the top. **A′:** Transverse section of a HH1 chicken embryo showing cshisa expression exclusively in the hypoblast. **B,B′:** Stage HH3$^+$ embryo showing expression of *cshisa* restricted to the endodermal layer. **C:** At HH5, *cshisa* transcripts are expressed in the prospective neural plate. **C′,C″,C‴:** Transverse sections of the embryo in C showing cShisa staining in endoderm and ectoderm. **D:** At HH6, *cshisa* expression appears restricted to the neural plate and primitive folds. **D′,D″:** Transverse sections a HH6 embryo show that cshisa transcripts are located in the ectodermal cells. **E:** In stage HH9, *cshisa* is expressed in the head folds and the somites. There is an absence of *cshisa* transcripts within the presomitic mesoderm of the embryo. **E′:** Section taken at the level of the somites shows *cshisa* expression within the somite and in the lateral plate mesoderm. The notochord is also positive for *cshisa* expression. **F:** At HH11, *cshisa* transcripts are observed in the forming brain, prospective eye, and at the somite level. In the somites, *cshisa* expression is strongest in the recently formed somites. **G:** By stage HH18, *cshisa* can be detected in the forebrain, eye, otic vesicle, pharyngeal pouches, branchial arches, somites, and the developing limb buds. **H:** *cshisa* expression in HH25 remains in the otic vesicle, forebrain, branchial arches, eye, somites, and limb buds. **H′,H″:** Transverse sections show that cshisa transcripts in the somite are restricted to the dermatome. **I,J:** cshisa expression in the early limb buds (J, stage HH22; I, stage HH25) has a very dynamic pattern. cshisa starts to be expressed more posteriorly and then migrates toward more distal region. Forelimbs are shown in the top and hindlimbs in the bottom. ba, branchial arches; dt, dermatome; ey, eye; fb, forebrain; hf, head fold; hyp, hypoblast; lpm, lateral plate mesoderm; ov, otic vesicle; nc, notochord; np, neural plate; pm, presomitic mesoderm; s, somite.

portance they may have during embryonic development of the mouse and chick embryos, patterning topologically equivalent regions in these vertebrate embryos.

Assuming, based on their homology with the *Xenopus* protein, that the mouse and chicken Shisa also function as antagonists of Wnt and FGF signalling, then their expression in the AVE and hypoblast may seem, at a first glance, hard to conciliate with the role attributed to these tissues in early neural induction. In fact, recent findings strongly suggest that, at least in chicken, FGF and Wnt signalling are required for neural induction at a very early stage, even before gastrulation. However, it should be taken into consideration that Shisa acts cell-autonomously; therefore, its expression in the AVE/hypoblast is unlikely to inhibit FGF signalling in the overlying epiblast. Shisa might instead play an indirect role in promoting neural induction by participating in the specification and/or maintenance of the AVE/hypoblast identities, for example through repression of the autocrine action of FGF-8, which is expressed in the AVE (Crossley and Martin, 1995). Later on, Shisa is expressed in the neural plate, and it's plausible then that, like in *Xenopus*, it inhibits the caudalizing Wnt and FGF signals in this tissue. A similar reasoning can be applied to the function of Shisa in the developing limb buds, where Wnt and FGF signaling is known to direct outgrowth and patterning. *shisa* is expressed in the ectoderm layer of the limbs, where most of the Wnt and FGF signalling centers are also located. Again it is conceivable that Shisa is not antagonizing these signalling pathways in the target mesenchymal cells but is instead acting on some of the signalling centers, perhaps protecting them from their own signals. During somitogenesis Shisa might be involved in the process of somite differentiation and condensation through the inhibition the FGF signalling coming from the posterior presomitic mesoderm. Subsequently expression in the dorsolateral compartment of the somite suggests that Shisa could be repressing the FGF- and Wnt-mediated myogenic signals in these cells, which as a result will be specified as dermatome. These considerations are purely hypothetical, however, and a more conclusive characterization of the biological function of the mouse and chicken Shisa in embryonic development will require further biochemical and genetic analyses.

EXPERIMENTAL PROCEDURES

Chicken and Mouse Embryo Collection

Fertilized chicken eggs were purchased from local suppliers. Eggs were incubated at 37°C in a humidified incubator until the desired developmental stage. Embryos were staged according to Hamburger and Hamilton (1951).

Mouse embryos were obtained crossing B6SJL/F1 hybrids maintained on a 19-hour light to 5-hour dark cycle and mated overnight. Noon of the day of vaginal plug detection was designated 0.5 dpc. Embryos were dissected from the uterus in phosphate buffered saline and further staged by morphological landmarks (Downs and Davies, 1993).

Cloning of *mshisa* and *cshisa* cDNAs

The EST clone BC057640, containing the entire predicted coding sequence of *mshisa* as well as the 5′- and 3′-UTRs, was obtained from RZPD (IMAGp998G149268Q3). To isolate a fragment of the *cshisa* coding sequence (323–829), total RNA from stage HH22 chick embryos (Hamburger and Hamilton, 1951) was isolated using Trizol reagent (Invitrogen) according to the manufacturer's protocol. Random-primed cDNA synthesized from these samples with H minus M-MuLV reverse transcriptase (Fermentas) was subjected to 25 cycles of amplification by polymerase chain reaction (PCR), at an annealing temperature of 55°C. The following primers were used: forward, 5′- CATTGTCGGCTCCGTCTTCGTC-3′; reverse, 5′-TTCTGCTCTCCGCCTGCATG -3′. The PCR product was cloned into the pGEM-T Easy vector (Promega). The sequence of PCR-amplified *cshisa* cDNA was determined on an ABI sequencer. The sequence of chicken *shisa* cDNA was deposited in the GenBank database under the accession no. DQ342343.

Whole-Mount In Situ Hybridization and Histology

Single whole-mount in situ hybridization and antisense-probe preparation were performed as previously described (Belo et al., 1997). Digoxigenin-labeled *mshisa* antisense RNA probe was synthesized by linearizing the BC05764 clone with *Bgl*II and transcribing with T7 RNA polymerase. To generate the digoxigenin-labeled *cshisa* antisense RNA probe, the plasmid containing *cshisa* coding sequence fragment (pGEM-Teasy.*cshisa*) was linearized using *Sal*I and transcribed using T7 RNA polymerase.

After staining, embryos were refixed in 4% paraformaldehyde and photographed by using a Leica DFCM20 digital camera. Some embryos were embedded in 15% sucrose, 7.5% gelatin, frozen, and sectioned (16 μm) using a Leica CMM0S0 S cryostat; others were embedded in paraffin and sectioned (8 μm) using a microtome Leica RM2135. The sections were examined and photographed using a Leica DM LB2 microscope and a Leica DFCM20 digital camera.

ACKNOWLEDGMENTS

We thank Ana T. Tavares and Nuno Afonso for critically reading of this manuscript. M.F., L.G., and A.C.S. are recipients of F.C.T. PhD fellowships. M.B. is recipient of a F.C.T. fellowship. This work was supported by research grants from F.C.T. and IGC/Fundação Calouste Gulbenkian to J.A.B., where he is a Principal Investigator.

REFERENCES

Altschul SF, Gish W, Miller W, Myers EW, Lipman DJ. 1990. Basic local alignment search tool. J Mol Biol 215:403–410.

Aulehla A, Herrmann BG. 2004. Segmentation in vertebrates: clock and gradient finally joined. Genes Dev 18:2060–2067.

Aulehla A, Wehrle C, Brand-Saberi B, Kemler R, Gossler A, Kanzler B, Herrmann BG. 2003. Wnt3a plays a major role in the segmentation clock controlling somitogenesis. Dev Cell 4:395–406.

Beddington RS, Robertson EJ. 1999. Axis development and early asymmetry in mammals. Cell 96:195–209.

Belo JA, Bouwmeester T, Leyns L, Kertesz N, Gallo M, Follettie M, De Robertis EM. 1997. Cereberus-like is a secreted factor with neutralizing activity expressed in the anterior-primitive endoderm of the mouse gastrula. Mech Dev 68:45–57.

Birney E, Andrews D, Caccamo M, Chen Y, Clarke L, Coates G, Cox T, Cunningham F, Curwen V, Cutts T, Down T, Durbin R, Fernandez-Suarez XM, Flicek P, Gräf S, Hammond M, Herrero J, Howe K, Iyer V, Jekosch K, Kähäri A, Kasprzyk A, Keefe D, Kokocinski F, Kulesha E, London D, Longden I, Melsopp C, Meidl P, Overduin B, Parker A, Proctor G, Prlic A, Rae M, Rios D, Redmond S, Schuster M, Sealy I, Searle S, Severin J, Slater G, Smedley D, Smith J, Stabenau A, Stalker J, Trevanion S, Ureta-Vidal A, Vogel J, White S, Woodwark C, Hubbard TJP. 2006. Ensembl 2006. Nucleic Acids Res 34:D556–D561.

Bouwmeester T, Leyns L. 1997. Vertebrate head induction by anterior primative endoderm. BioEssays 19:855–863.

Burge C, Karlin S. 1997. Prediction of complete gene structures in human genomic DNA. J Mol Biol 268:78.

Capdevila J, Izpisua Belmonte JC. 2001. Patterning mechanisms controlling vertebrate limb development. Annu Rev Cell Dev Biol 17:87–132.

Crossley PH, Martin GR. 1995. The mouse Fgf8 gene encodes a family of polypeptides and is expressed in regions that direct outgrowth and patterning in the developing embryo. Development 121:439.

Deng CX, Wynshaw-Boris A, Shen MM, Daugherty C, Ornitz DM, Leder P. 1994. Murine FGFR-1 is required for early postimplantation growth and axial organization. Genes Dev 8:3045–3057.

Downs KM, Davies T. 1993. Staging of gastrulating mouse embryos by morphological landmarks in the dissecting microscope. Development 118:1255–1266.

Dubrulle J, Pourquie O. 2004a. Coupling segmentation to axis formation. Development 131:5783–5793.

Dubrulle J, Pourquie O. 2004b. fgf8 mRNA decay establishes a gradient that couples axial elongation to patterning in the vertebrate embryo. Nature 427:419–422.

Dubrulle J, McGrew MJ, Pourquie O. 2001. FGF signaling controls somite boundary position and regulates segmentation clock control of spatiotemporal Hox gene activation. Cell 106:219–232.

Foley AC, Skromne I, Stern CD. 2000. Reconciling different models of forebrain induction and patterning: a dual role for the hypoblast. Development 127:3839–3854.

Gamer LW, Cox KA, Small C, Rosen V. 2001. Gdf11 is a negative regulator of chondrogenesis and myogenesis in the developing chick limb. Dev Biol 229:407–420.

Glinka A, Wu W, Onichtchouk D, Blumenstock C, Niehrs C. 1997. Head induction by simultaneous repression of Bmp and Wnt signalling in Xenopus. Nature 389: 517–519.

Glinka A, Wu W, Delius H, Monaghan AP, Blumenstock C, Niehrs C. 1998. Dickkopf-1 is a member of a new family of secreted proteins and functions in head induction. Nature 391:357–362.

Grass S, Arnold HH, Braun T. 1996. Alterations in somite patterning of Myf-5-deficient mice: a possible role for FGF-4 and FGF-6. Development 122:141.

Hamburger V, Hamilton HL. 1951. A series of normal stages in the development of the chick embryo. J Morphol 88:49–92.

Katoh Y, Katoh M. 2005. Comparative genomics on Shisa orthologs. Int J Mol Med 16:181.

Mangold O. 1933. Über die Induktionsfähigkeit der verschiedenen Bezirke der Neurula von Urodelen. Naturwissenschaften 21:761–766.

Mao B, Wu W, Li Y, Hoppe D, Stannek P, Glinka A, Niehrs C. 2001. LDL-receptor-related protein 6 is a receptor for Dickkopf proteins. Nature 411:321–325.

Mesnard D, Filipe M, Belo JA, Zernicka-Goetz M. 2004. The anterior-posterior axis emerges respecting the morphology of the mouse embryo that changes and aligns with the uterus before gastrulation. Curr Biol 14:184–196.

Oulad-Abdelghani M, Chazaud C, Bouillet P, Mattei MG, Dolle P, Chambon P. 1998. Stra3/lefty, a retinoic acid-inducible novel member of the transforming growth factor-beta superfamily. Int J Dev Biol 42:23–32.

Pfeffer PL, De Robertis EM, Izpisua-Belmonte JC. 1997. Crescent, a novel chick gene encoding a Frizzled-like cysteine-rich domain, is expressed in anterior regions during early embryogenesis. Int J Dev Biol 41:449–458.

Piccolo S, Sasai Y, Lu B, De Robertis EM. 1996. Dorsoventral patterning in Xenopus: inhibition of ventral signals by direct binding of chordin to BMP-4. Cell 86:589–598.

Piccolo S, Agius E, Leyns L, Bhattacharyya S, Grunz H, Bouwmeester T, De Robertis EM. 1999. The head inducer Cereberus is a multifunctional antagonist of Nodal, BMP and Wnt signals. Nature 397:707–710.

Pirskanen A, Kiefer JC, Hauschka SD. 2000. IGFs, insulin, Shh, bFGF, and TGF-beta1 interact synergistically to promote somite myogenesis in vitro. Dev Biol 224:189.

Pourquie O. 2001. Vertebrate somitogenesis. Annu Rev Cell Dev Biol 17:311–350.

Pourquie O. 2004. The chick embryo: a leading model in somitogenesis studies. Mech Dev 121:1069–1079.

Rivera-Perez JA, Mager J, Magnuson T. 2003. Dynamic morphogenetic events characterize the mouse visceral endoderm. Dev Biol 261:470–487.

Rodriguez TA, Srinivas S, Clements MP, Smith JC, Beddington RS. 2005. Induction and migration of the anterior visceral endoderm is regulated by the extra-embryonic ectoderm. Development 132: 2513–2520.

Rodriguez Esteban C, Capdevila J, Economides AN, Pascual J, Ortiz A, Izpisua Belmonte JC. 1999. The novel Cer-like protein Caronte mediates the establishment of embryonic left-right asymmetry. Nature 401:243–251.

Silva AC, Filipe M, Kuerner KM, Steinbeisser H, Belo JA. 2003. Endogenous Cereberus activity is required for anterior head specification in Xenopus. Development 130:4943–4953.

Spemann H. 1931. Über den Anteil von Implantat und Wirtskeim an der Orientierung und Beschaffenheit der induzierten Embryonalanlage. W Roux Arch Entwicklungsmech 123:390–516.

Srinivas S, Rodriguez T, Clements M, Smith JC, Beddington RS. 2004. Active cell migration drives the unilateral movements of the anterior visceral endoderm. Development 131:1157–1164.

Stern HM, Hauschka SD. 1995. Neural tube and notochord promote in vitro myogenesis in single somite explants. Dev Biol 167:87.

Sun X, Meyers EN, Lewandoski M, Martin GR. 1999. Targeted disruption of Fgf8 causes failure of cell migration in the gastrulating mouse embryo. Genes Dev 13:1834–1846.

Thomas P, Beddington R. 1996. Anterior primitive endoderm may be responsible for patterning the anterior neural plate in the mouse embryo. Curr Biol 6:1487–1496.

Wagner J, Schmidt C, Nikowits W Jr, Christ B. 2000.Compartmentalization of the somite and myogenesis in chick embryos are influenced by wnt expression. Dev Biol 228:86.

Yamamoto M, Saijoh Y, Perea-Gomez A, Shawlot W, Behringer RR, Ang SL, Hamada H, Meno C. 2004. Nodal antagonists regulate formation of the anteroposterior axis of the mouse embryo. Nature 428:387–392.

Yamamoto A, Nagano T, Takehara S, Hibi M, Aizawa S. 2005. Shisa promotes head formation through the inhibition of receptor protein maturation for the caudalizing factors, Wnt and FGF. Cell 120:223–235.

Yoshikawa Y, Fujimori T, McMahon AP, Takada S. 1997. Evidence that absence of Wnt-3a signaling promotes neuralization instead of paraxial mesoderm development in the mouse. Dev Biol 183:234–242.

Zimmerman LB, De Jesus-Escobar JM, Harland RM. 1996. The Spemann organizer signal noggin binds and inactivates bone morphogenetic protein 4. Cell 86: 599–606.